

Technical aspects of quantum chemical modeling of enzymatic reactions: the case of phosphotriesterase

Shi-Lu Chen · Wei-Hai Fang · Fahmi Himo

Received: 8 October 2007 / Accepted: 16 February 2008 / Published online: 7 March 2008
© Springer-Verlag 2008

Abstract Quantum chemical methods are today a powerful tool in the study of enzymatic reaction mechanisms. In this paper we evaluate the adequacy of some of the technical approximations frequently used in the modeling of enzyme reactions with high level methods. These include the choice of basis set for geometry optimizations and energy evaluation, the choice of dielectric constant to model the enzyme surrounding, and the effects of locking the centers of truncation. As a test case, we choose the phosphotriesterase enzyme, which is a binuclear zinc enzyme that catalyzes the hydrolysis of organophosphate triesters.

1 Introduction

Advancements in density functional methods, in particular the development of the B3LYP functional, coupled with the nearly exponential growth of computer power, have made it possible to treat ever larger systems at a reasonable level of accuracy. Using the B3LYP functional with a medium-sized basis set, one can today routinely handle systems containing more than 100 atoms, a development that has opened the door for many applications. One of the fields that quantum chemical methods have had very positive impacts on in recent years is the study of enzymatic reaction mechanisms. Many researchers have used DFT methods to investigate mechanis-

tic aspects of a wide range of different enzymes and enzyme families [1–24].

When investigating mechanistic proposals, one has to perform a large number of calculations to find different transition states and intermediates to test the various scenarios. Consequently, the computational scheme used has to be fast and robust enough to allow this. At the same time, the accuracy of the approximations made in the models has to be higher than or comparable to the accuracy of the underlying computational scheme (in this case the B3LYP functional).

One very fruitful approach has been to cut out a relatively small model of enzyme around the active site and treat it at a quite high level of theory. To model the parts of the enzyme that are not included in the quantum model, two main approximations have been used. To account for the polarization effects, the enzyme surrounding can, to a first approximation, be considered as a homogenous polarizable medium which can be modeled using some dielectric cavity techniques. In this model, the solvent is represented by a constant dielectric medium surrounding a cavity containing the active site. The solvation energies are usually calculated as single points on top of the optimized geometries.

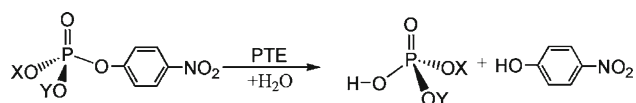
In addition to the polarization effect, the ignored enzyme surrounding can also impose steric effect on the active site, forcing various groups to stay in certain positions or preventing them from making certain movements. In order to keep the various groups in place to as much as possible resemble the crystal structure, certain atoms in the model, typically where the truncation is made, are kept fixed to their X-ray positions during the geometry optimizations. If done properly, this approach will ensure the structural integrity of the model, yet allowing for some flexibility of various groups.

The combination of continuum solvation and the coordinate-locking scheme represents a quite simple but yet

Contribution to the Nino Russo Special Issue.

S.-L. Chen · F. Himo (✉)
Department of Theoretical Chemistry, School of Biotechnology,
Royal Institute of Technology, 10691 Stockholm, Sweden
e-mail: himo@theochem.kth.se

S.-L. Chen · W.-H. Fang
College of Chemistry, Beijing Normal University, 100875 Beijing,
People's Republic of China



Scheme 1 The hydrolysis reaction of organophosphate triesters catalyzed by PTE. *X* and *Y* are alkyl substituents

powerful way to account for the parts of the enzyme that are not included in the model. It can easily be seen that both these approximations become more and more accurate as the quantum chemical models of the active site get larger and larger. A larger active site model already contains at the quantum level most of the polarization around the reactive parts of the enzyme. Also, when constraining the centers of truncation in a large active site model, enough flexibility is granted to the various groups to resemble the enzyme. The energies calculated with this modeling scheme have proven to be accurate enough to test mechanistic proposals, i.e. the energies are often sufficient to substantiate or rule out a suggested reaction mechanism.

In the present paper, we further investigate the adequacy of some of the technical details involved in this kind of modeling, including the choice of basis set used in the geometry optimization and energy evaluation, the choice of dielectric constant for the solvation calculations, and the effect of imposing constraints on the truncation points. The specific enzyme under consideration is phosphotriesterase (PTE). PTE is a bacterial enzyme that catalyzes the hydrolysis of organophosphate triesters (Scheme 1) [25,26], some of which are employed as agricultural insecticides and chemical warfare nerve agents and counted among the most dangerous compounds ever synthesized [27,28]. No naturally occurring substrate for PTE has been found to date [29], which has led to the assumption that the catalytic activity has only recently evolved due to the wide-spread use of insecticides [30].

PTE is a homodimer with each subunit containing a divalent bimetallic active site [31,32]. In the native enzyme, the metal ions are zinc ions. Interestingly, the two zinc ions can be replaced by Cd^{2+} , Ni^{2+} , Co^{2+} , and Mn^{2+} ions without complete loss of enzymatic activity [33]. The two zinc ions (α -Zn and β -Zn) are located at a distance of $\sim 3.4 \text{ \AA}$ from each other and are connected to the protein matrix via the side chains of His55, His57, His201, His230, and Asp301.

Scheme 2 Proposed reaction mechanism of phosphotriesterase

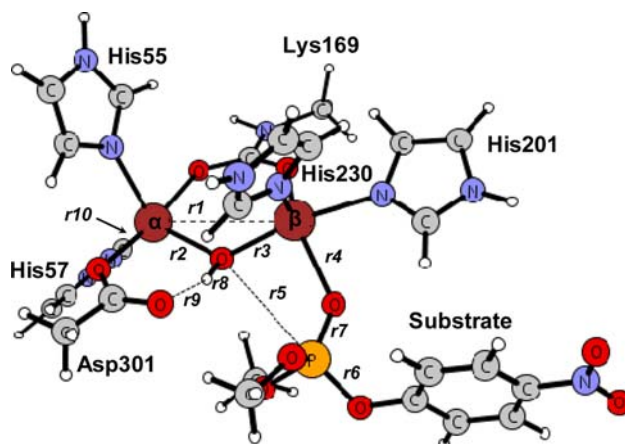
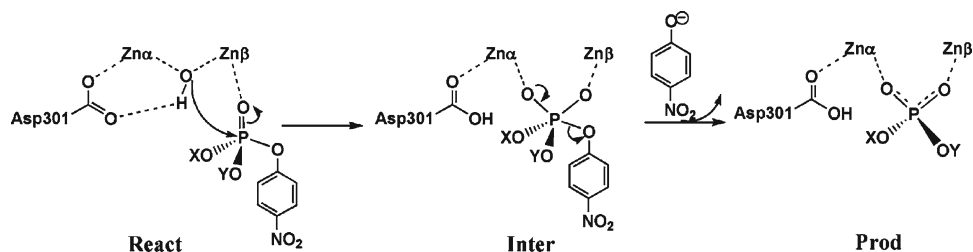


Fig. 1 Model of the PTE active site used in the present investigation. Key bond distances are defined

A hydroxide and a carboxylated lysine residue (Lys169) bridge the two zinc ions [34].

We have very recently used the quantum chemical approach outlined above to investigate the mechanism of this enzyme [35]. We used a model consisting of 82 atoms, as shown in Fig. 1, to calculate the potential energy curve for the hydrolysis of the 4-nitrophenyl-phosphate substrate. The calculations gave support to the reaction mechanism shown in Scheme 2, which is consistent with all biochemical, kinetic, and spectroscopic data available for this enzyme [36,37]. In this mechanism, the bridging hydroxide performs a nucleophilic attack on the substrate from its bridging position to form a penta-coordinated intermediate. Next, this intermediate collapses and the leaving group departs. For this substrate, no activation (protonation) of the leaving group was found to be necessary. The second step was found to be the rate-limiting step and the role of the β -Zn was argued to be to stabilize the intermediate and product species, thereby lowering the barriers for the nucleophilic attack and the P–O bond cleavage [35].

In the present paper, we will not discuss the mechanism of PTE any further. We will rather focus on some of the technical issues involved in the calculation of the potential energy profile for the enzyme. The results should be of importance when modeling other metalloenzymes, in particular other members of the family of binuclear Zn enzymes.

2 Computational details

All calculations were performed using the density functional theory (DFT) functional B3LYP [38–40] as implemented in the Gaussian03 program package [41].

As will be discussed below, geometry optimizations were carried out with two different basis sets. In the first, the 6-31G(d,p) basis set was used for all atoms except the Zn, for which the LANL2DZ basis set was used. In the second geometry optimization the same basis set as the first was used except for the phosphorus center and the five oxygen atoms around it (the attacking oxygen, the leaving oxygen, and the other three directly-coordinated oxygens), for which the 6-311+G(2d) basis set was used.

The final energy were obtained by a single point calculation using the optimized geometry and the 6-311+G(2d,2p) basis set.

Solvation effects were calculated at the same theory level as the optimizations by performing single point calculations on the optimized structures using the CPCM method [42–45]. Two dielectric constants were used, $\epsilon = 4$ and $\epsilon = 80$.

Frequency calculations were performed at the same theory level as the optimizations to obtain zero-point energies (ZPE) and to confirm the nature of the stationary points. The latter implies no negative eigenvalues for minima and only one negative eigenvalue for transition states. For the geometry optimization performed with the larger basis set, the ZPE were taken from the calculations with the smaller basis set.

As will be discussed below, in one of the models, some atoms were kept fixed to their X-ray crystal positions to study the effect of such a constraining scheme on the energetics. This procedure gives rise to a few small imaginary frequencies, typically on the order of 10 cm^{-1} . These frequencies do not contribute significantly to the ZPE and can thus be ignored.

3 Results and discussion

3.1 Active-site model

The quantum chemical model used in the present investigation is the same as the one we used in the previous study [35]. It consists of two zinc ions and their first shell ligands, including the bridging hydroxide (O_μH^-), the four histidines (His55, His57, His201, His230), the Asp301, and the carboxylated Lys169. Coordinates were taken from the high resolution crystal structure (PDB code 1HZY, 1.30 Å resolution) [34] and hydrogen atoms were added manually. The ligands were truncated so that in principle only side chains were kept in the model. The histidines were thus represented by imidazoles, the aspartate by an acetate, and the carboxylated lysine by a carboxylated methylamine. As a substrate,

we use, as in the previous study, the dimethyl 4-nitrophenyl phosphate. The phosphoryl oxygen of the substrate binds to the more solvent-exposed β -Zn site and the leaving group is located at the position opposite to the nucleophile (O_μH^-). The total number of atoms of the model is 82 and the total charge is +1.

3.2 Effect of basis set

It is a common procedure in quantum chemical studies to first optimize the geometries of the stationary points using a medium-sized basis set and then apply a much larger basis set as a single point calculation to evaluate the energetics.

In this study, we have first optimized the geometries using the LANL2DZ basis set on the zinc ions and 6-31G(d,p) on all other atoms. Hereafter, this will be called Basis Set 1 (BS1). The optimized structures of the stationary points along the reaction pathway using BS1 are presented in Fig. 2, and the most important geometric parameters are listed in Table 1.

We first note that the overall geometric parameters obtained from the geometry optimization of the reactant structure (**React**) agree very well with the X-ray structure. For example, the bond distances of the bridging oxygen to the two zinc ions are calculated to be 2.00 and 1.99 Å, to be compared to the crystallographic distances of 2.0 Å [34]. The calculated Zn–Zn distance is 3.42 Å, which is also very close to the crystallographic distance of ~ 3.4 Å [34].

The resulting potential energy curve using BS1 is shown in Fig. 3. The nucleophilic attack by the bridging O_μH^- on the substrate is calculated to have a barrier of 8.2 kcal/mol (**TS1**) and the resulting penta-coordinated intermediate (**Inter**) is calculated to lie at +5.2 kcal/mol relative to the **React**. From **Inter**, the barrier for the dissociation and the departure of the leaving group (**TS2**) is 5.4 kcal/mol (+10.6 kcal/mol relative to **React**) and the resulting product (**Prod**) is 0.8 kcal/mol lower than **React**.

When applying a larger basis set (LBS: 6-311+G(2d,2p) on all atoms) as a single point energy calculation on the optimized geometries, some significant changes are observed on the potential energy surface. The energies of **TS1**, **Inter**, and **TS2** is raised relative to **React**, while the energy of **Prod** is lowered. For **Inter**, the increase in energy is 6.7 kcal/mol (from 5.2 to 11.9 kcal/mol), while for **TS1** and **TS2** the raise is ca 3 kcal/mol. In fact, using this basis set, the energy of the intermediate becomes slightly higher (0.2 kcal/mol) than the energy of **TS1**, which is of course an artifact of the procedure used. These results indicate that the small basis set (BS1) is not adequate for a proper description of the changes that take place during the reaction, and thus a larger basis set is needed to obtain reliable energetics.

This raises the question whether a large basis set is also required to obtain reliable geometries. It is commonly argued that for reactions involving phosphates, a larger basis set

Fig. 2 Optimized structures of the stationary points along the reaction pathway using Basis Set I

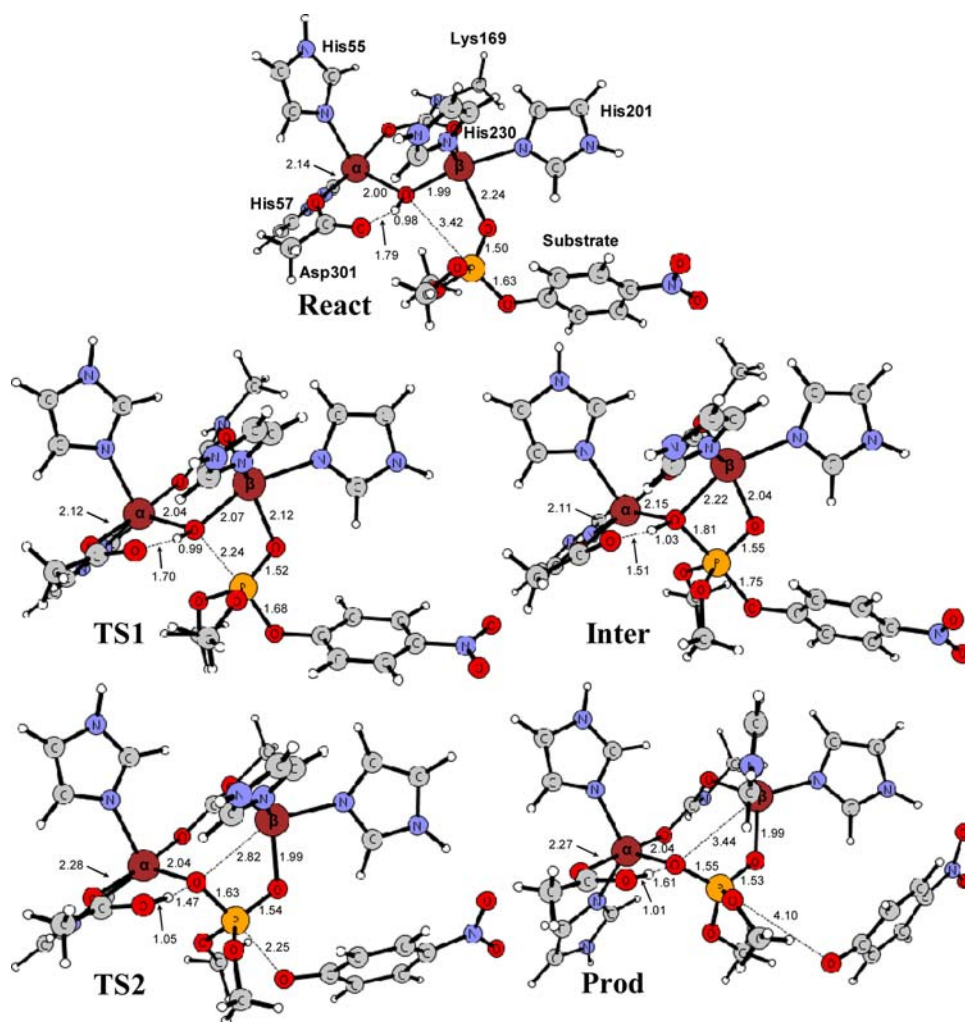


Table 1 Important geometric parameters for the various stationary points using different models

	React			TS1			Inter			TS2			Prod		
	BS1	BS2	F	BS1	BS2	F	BS1	BS2	F	BS1	BS2	F	BS1	BS2	F
r_1	3.54	3.53	3.41	3.49	3.55	3.41	3.69	3.71	3.46	3.95	3.92	3.43	4.34	4.36	3.59
r_2	2.00	2.00	1.97	2.04	2.06	2.03	2.15	2.14	2.07	2.04	2.04	2.02	2.04	2.04	2.03
r_3	1.99	1.98	2.01	2.07	2.10	2.11	2.22	2.22	2.16	2.82	2.74	2.28	3.44	3.46	2.64
r_4	2.24	2.28	2.20	2.12	2.08	2.09	2.04	2.02	2.05	1.99	1.98	2.06	1.99	1.98	2.03
r_5	3.42	3.45	3.00	2.24	2.12	2.07	1.81	1.81	1.86	1.63	1.62	1.64	1.55	1.53	1.57
r_6	1.63	1.62	1.64	1.68	1.68	1.70	1.75	1.74	1.73	2.25	2.16	2.35	4.10	4.24	3.79
r_7	1.50	1.48	1.50	1.52	1.51	1.53	1.55	1.53	1.54	1.54	1.53	1.53	1.53	1.51	1.52
r_8	0.98	0.98	0.98	0.99	0.99	1.10	1.03	1.02	1.04	1.47	1.48	1.52	1.61	1.63	1.58
r_9	1.79	1.81	1.86	1.70	1.68	1.65	1.51	1.56	1.51	1.05	1.05	1.03	1.01	1.01	1.01
r_{10}	2.14	2.14	2.16	2.12	2.12	2.15	2.11	2.11	2.14	2.28	2.29	2.27	2.27	2.29	2.28

The parameters are defined in Fig. 1, BS1 LANL2DZ on Zn and 6-31G(d,p) on all other atoms, BS2 same as BS1 but using 6-311+G(2d) on the phosphorous center and the five oxygens around it, F the model in which the truncation atoms are fixed

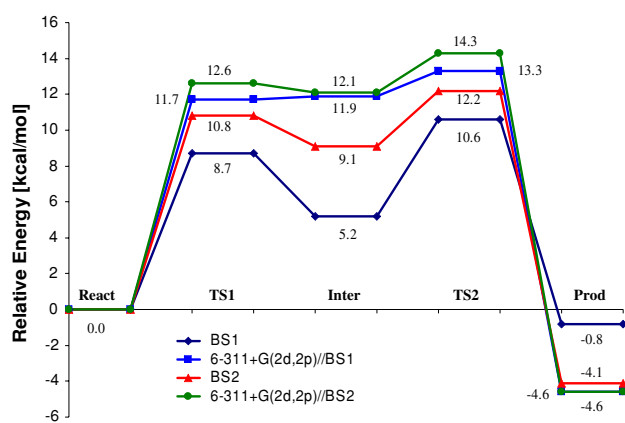


Fig. 3 Calculated potential energy profile for the PTE reaction using different basis sets. *BS1*: LANL2DZ on Zn and 6-31G(d,p) on all other atoms. *BS2*: Same as *BS1* but using 6-311+G(2d) on the phosphorous and the five oxygens around it

on these atoms should be used in the geometry optimizations, typically including polarization and diffuse functions. To investigate this issue, we have re-optimized all the geometries using the same basis set as before (*BS1*), but with the important difference that for the phosphor center and all five oxygens around it the 6-311+G(2d) was used. This combination will be called Basis Set 2 (*BS2*).

The calculated potential energy curve using this basis set is displayed in Fig. 3, and the most important geometric parameters are listed in Table 1.

As expected, the geometry optimization with the larger basis set leads to some changes in the geometries around the phosphor center. The largest changes are seen for the forming O_{μ} -P bond in *TS1*, and the breaking P- O_L bond in *TS2*, both of which are contracted by ca 0.1 Å. The rest of the changes are more modest.

The better description of the phosphor center and its surrounding atoms leads to a considerable difference in the energetics compared to *BS1*. The energies obtained with *BS2* are now much closer to the ones obtained by *LBS//BS1* than the ones obtained with *BS1* (see Fig. 3). For example, the barrier for the first step is calculated to be 10.8 kcal/mol with *BS2* compared to 8.7 and 11.7 kcal/mol for *BS1* and *LBS//BS1*, respectively. The other stationary point shows similar behavior.

However, a very important result here is that when applying the large basis set on the *BS2*-optimized geometries, the potential energy curve is very similar to the one obtained by applying the large basis set on the *BS1*-optimized geometries (see Fig. 3). The differences are less than 1 kcal/mol. There is thus no big advantage in using a larger basis set for the geometry optimizations, even for reactions involving phosphate hydrolysis, like the one in PTE.

In summary, the results presented above demonstrate that geometries can be optimized using a medium-sized basis set,

while the final energies should definitely be evaluated using a much larger basis set.

3.3 Choice of dielectric constant

As discussed in Introduction, a relatively cheap way to estimate the energetic effects of the parts of the enzyme that are not included in the quantum chemical model is to assume that it is a homogenous medium, with some assumed dielectric constants ϵ . This strategy has been used frequently in quantum chemical modeling of enzymatic reactions [1–24]. The choice of the dielectric constant is somewhat arbitrary, but the value of $\epsilon = 4$ is often used for protein surrounding.

To investigate what effect the choice of the dielectric constant has on the energetics, we have used two different values, $\epsilon = 4$ and $\epsilon = 80$. The solvent effects are calculated as single point corrections at the same level of theory as the geometry optimizations. We have done this using both the *BS1*- and *BS2*-optimized geometries and added the effect to the energies obtained from the large basis set calculations. The results are shown in Fig. 4.

As seen from Fig. 4, solvation effects do not change the energetics of the first step significantly. The barrier calculated at the *LBS//BS1* level, for example, is slightly reduced from 11.7 to 10.8 and 10.5 kcal/mol, upon addition of dielectric effects using $\epsilon = 4$ and $\epsilon = 80$, respectively. Similarly, the energy of the intermediate is lowered from 11.9 to 9.7 and 8.9 kcal/mol, respectively.

In the second step, however, the solvation effects are more pronounced. The barrier is lowered by 1.6 and 2.2 kcal/mol using $\epsilon = 4$ and $\epsilon = 80$, respectively. More significantly, the energy of the product is lowered by as much as 8.0 and 10.7 kcal/mol, with $\epsilon = 4$ and $\epsilon = 80$, respectively. Although it is a very large effect, it is easy to rationalize these results considering that the P-O bond cleavage of the second step results in an anionic phenolate product that dissociates from the active site. Upon addition of dielectric solvation, the energy of this species will, of course, be lowered considerably more than the other stationary points. Very similar solvation effects on the potential energy curve are observed when using *BS2* (Fig. 4, right panel).

As expected, the solvation effects saturate very quickly as a function of the dielectric constant. In going from the cluster model ($\epsilon = 1$) to $\epsilon = 4$, most of the solvation is accounted for. The difference between $\epsilon = 4$ and $\epsilon = 80$ is not very large. This result can easily be rationalized by considering the simple Onsager model of a dipole in a spherical cavity, for which the solvation energy there is proportional to $(\epsilon - 1)/(2\epsilon + 1)$.

Most importantly, the choice of the dielectric constant does not change any conclusion drawn about the mechanism of the enzyme under consideration. Furthermore, a general conclusion from the calculations is that unless charges are

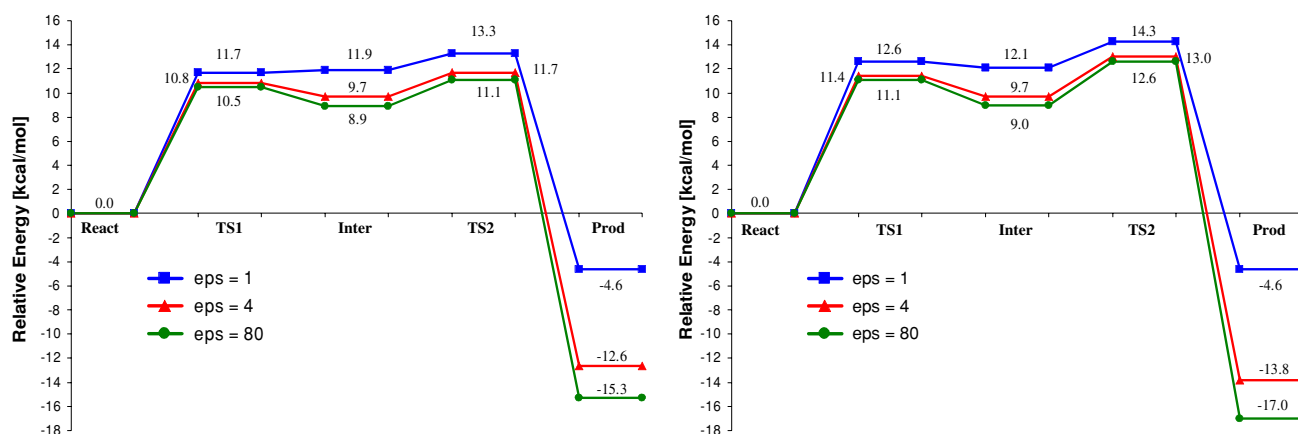


Fig. 4 Calculated potential energy profile for the PTE reaction using different dielectric constants. *Left* Geometries and solvation effects calculated with BS1. *Right* Geometries and solvation effects calculated with BS2

created or quenched close to the edge of the quantum model, the relative solvent effects between minima and transition states are usually quite small. These conclusions indicate that the exact choice of the dielectric constant is less critical in the quantum chemical modeling of enzyme active sites.

3.4 Effect of locking atoms

A common procedure in modeling enzymatic reactions using quantum chemical models of the active site is to fix the atoms to their crystallographic positions where the truncation is made. This is done to prevent the various groups from making large movements that they otherwise would not do if the rest of the enzyme is present. For metalloenzymes, this problem is less pronounced, since the metal ions usually anchor the various parts of the active site and prevents this kind of artificial movements. However, if there are some second-shell residues that need to be included in the model, or if the first-shell ligands can move and form favorable hydrogen bonds to each other, then fixing the truncation position can solve the problem. With this procedure, there is, however, a risk that the created model becomes too rigid and that the imposed strain will have a large effect on the energetics.

To examine how much this kind of procedure affects the relative energies of the reaction, we have re-done all the calculations for the PTE active site using the same model as above, but with the truncation centers fixed to their crystallographic positions. In total, six positions were kept fixed, as indicated by the stars in Fig. 5. The optimized geometries using this model (using basis set 1) are presented in Fig. 5 (summary in Table 1) and the resulting energetic profile (calculated at the 6-311+G(2d,2p)//BS1 level) is shown in Fig. 6.

As seen from Fig. 5 and Table 1, some significant differences can be observed between the constrained and unconstrained geometries. If we take the Zn–Zn distance (**r1**, see

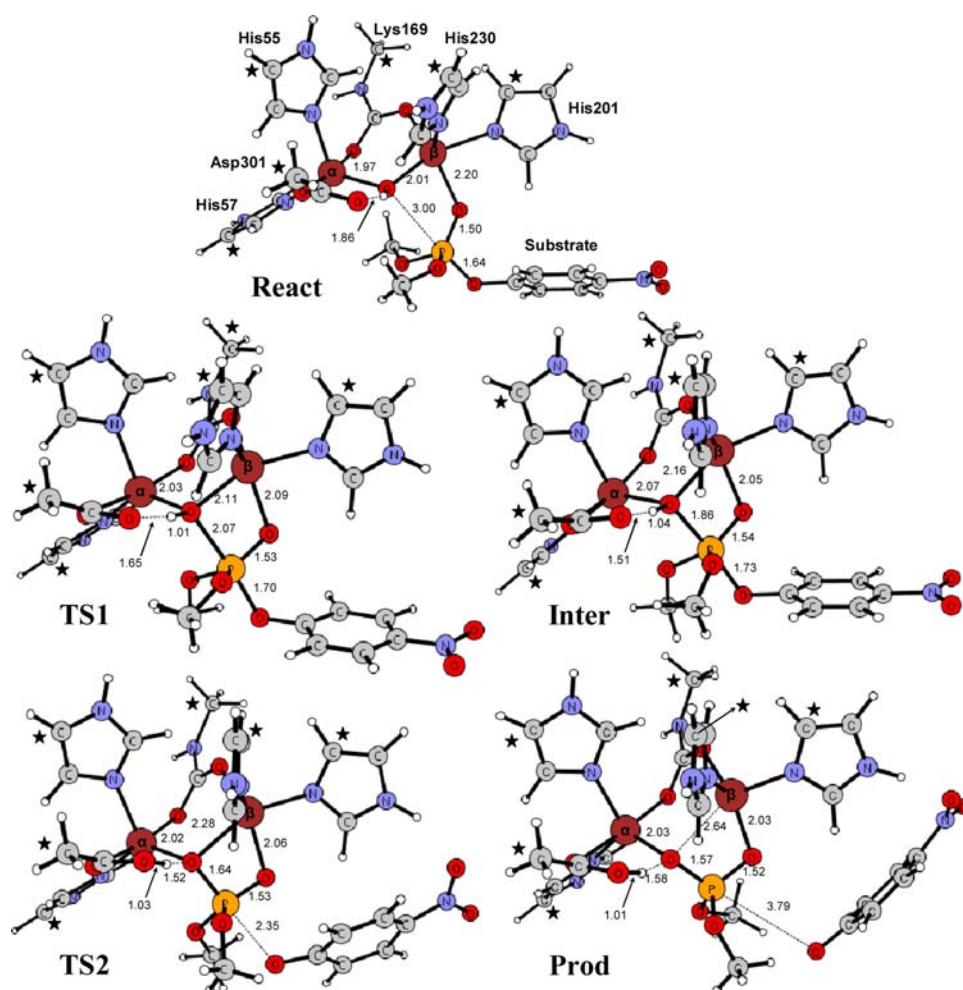
Fig. 1) as an indicator of the amount of strain imposed on the active site by the locking scheme, we can see that this strain is increasing in going from **React** to **Prod**. The Zn–Zn distance for the **React**, **Inter**, and **Prod** structures is 3.54, 3.69, and 4.34 Å, respectively, for the unconstrained model, to be compared to 3.41, 3.46, and 3.59 Å, respectively, for the constrained model. This indicates that there is larger amount of strain in the **Prod** compared to **React**. Another significant difference is seen for **r3**, the O_{μ} – Zn_{β} bond length, which is much more strained in **TS2** and **Prod** compared to **React**, which again indicates that there is larger amount of strain in the **Prod** compared to **React**. This strain is indeed reflected in the calculated energies. **Prod** is now 0.4 kcal/mol higher than **React**, compared to -4.6 kcal/mol in the unconstrained model. The strain thus caused a difference of 5.0 kcal/mol.

We can also observe significant changes in **r5**, the distance between the bridging oxygen and the phosphorous center of the substrate. In the **React** of the unconstrained model, **r5** is 3.42 Å, compared to 3.00 Å in the constrained model. The differences for the other stationary points are smaller, which suggests that the **React** species of the constrained model is more strained and destabilized compared to the other stationary point. Indeed, the energies of **TS1**, **Int**, and **TS2** are all shifted down compared to **React**, by 3.5, 3.7, and 2.1 kcal/mol, respectively.

Overall, locking the truncation atoms to their crystallographic positions seems to lead to a significant amount of strain, as judged by the geometric parameters (Table 1) and also the potential energy curves (Fig. 6) compared to the unconstrained model. However, these changes are not of such a magnitude that they will alter any conclusion about the mechanism of PTE. In particular, the change in the overall barrier of the rate-limiting step (**TS2**) is only about 2 kcal/mol.

It should here be said that the truncation applied in the present study is considered to be too tight. Today, it is not customary to truncate the histidines at the imidazole rings,

Fig. 5 Optimized structures of the stationary points along the reaction pathway with constraint. *Asterisks* indicate the atoms that are fixed to their X-ray positions



and lock atoms of the ring. At least one more carbon atom is kept in the model, which in this case would have led to more flexibility for the active site model, and hence less strain and less effects on the calculated energies.

4 Conclusions

In the present paper, we have investigated some technical aspects concerned with the quantum chemical modeling of enzymatic reactions. As a test case we chose to work with the phosphotriesterase enzyme, the mechanism of which we have recently investigated using the B3LYP functional [35]. The adequacy of three typical modeling approximations is evaluated with respect to the potential energy profiles.

It is concluded that geometries can be calculated using a medium-sized basis set without a significant loss of accuracy. However, the final energies should be evaluated using a quite large basis set, as this yields a considerably different PES.

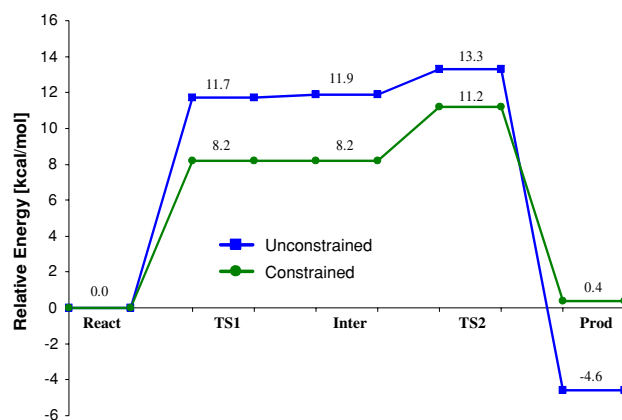


Fig. 6 Potential energy curves for the PTE reaction with and without constraints on the truncation atoms

Furthermore, it is concluded that the choice of the dielectric constant to compensate for the parts of the enzyme that are not included in the model is less critical, as the effect on the energy saturates very quickly with the dielectric constant.

For steps that do not involve creation of quenching of charge at the edge of the quantum model, the solvation effects are not very significant, while it is of huge importance when the charge state is changing at the edge of the mode, like for example the case of the departure of a charged leaving group.

A very simple way to model the steric effects imposed by the enzyme parts that are not included in the model is to lock the centers where the active site truncation is made. It is shown that this approximation can lead to a significant degree of strain if the model is not large enough. However, this was not found to change the conclusion drawn about the reaction mechanism in the case of PTE. Of course, as the size of the quantum model increases, the errors associated with both the homogenous continuum model and the coordinate-locking scheme will diminish, since most of the solvation will already be included in the quantum model and the model will have enough flexibility to accommodate changes of the geometry along the reaction path.

Acknowledgments F.H. gratefully acknowledges financial support from The Swedish National Research Council, The Wenner-Gren Foundations, The Carl Trygger Foundation, and The Magn Bergvall Foundation. This work was supported by grant from the Major State Basic Research Development Programs (Grant No. 2004CB719903) to W.-H.F.

References

- Siegbahn PEM, Blomberg MRA (2001) *J Phys Chem B* 105:9375
- Siegbahn PEM (2003) *Q Rev Biophys* 36:91
- Siegbahn PEM, Borowski T (2006) *Acc Chem Res* 39:729
- Himo F, Siegbahn PEM (2003) *Chem Rev* 103:2421
- Noodleman L, Lovell T, Han W-G, Li J, Himo F (2004) *Chem Rev* 104:459
- Himo F (2006) *Theor Chem Acc* 116:232
- Himo F (2005) *Biochim Biophys Acta—Bioenergetics* 1707:24
- Leopoldini M, Russo N, Toscano M (2007) *Chem Eur J* 13:2109
- Leopoldini M, Russo N, Toscano M, Dulak M, Wesolowski TA (2006) *Chem Eur J* 12:2532
- Marino T, Russo N, Toscano M (2005) *J Am Chem Soc* 127:4242
- Sousa SF, Fernandes PA, Ramos MJ (2007) *J Phys Chem B* 111:9146
- Sousa SF, Fernandes PA, Ramos MJ (2007) *J Am Chem Soc* 129:1378
- Cerqueira NMFS, Fernandes PA, Ramos MJ (2006) *J Phys Chem B* 110:21272
- Cerqueira NMFS, Fernandes PA, Eriksson LA, Ramos MJ (2006) *Biophys J* 90:2109
- Liu HN, Robinet JJ, Ananvoranich S, Gauld JW (2007) *J Phys Chem B* 111:439
- Cho K-B, Gauld JW (2005) *J Phys Chem B* 109:23706
- Hopmann KH, Hallberg BM, Himo F (2005) *J Am Chem Soc* 127:14339
- Himo F, Guo J-D, Rinaldo-Matthis A, Nordlund P (2005) *J Phys Chem B* 109:20004
- Velichkova P, Himo F (2005) *J Phys Chem B* 109:8216
- Velichkova P, Himo F (2006) *J Phys Chem B* 110:16
- Hopmann KH, Himo F (2006) *Chem Eur J* 12:6898
- Hopmann KH, Himo F (2006) *J Phys Chem B* 110:21299
- Sevastik R, Himo F (2007) *Bioorg Chem* 35:444
- Hopmann KH, Guo J-D, Himo F (2007) *Inorg Chem* 46:4850
- Dumas DP, Caldwell SR, Wild JR, Raushel FM (1989) *J Biol Chem* 264:19659
- Li W-S, Lum KT, Chen-Goodspeed M, Sogorb MA, Raushel FM (2001) *Bioorg Med Chem* 9:2083
- Hill CM, Li WS, Thoden JB, Holden HM, Raushel FM (2003) *J Am Chem Soc* 125:8990
- Russell AJ, Berberich JA, Drevon GF, Koepsel RR (2003) *Annu Rev Biomed Eng* 5:1
- Raushel FM, Holden HM (2000) *Adv Enzymol RMB* 74:51
- Buchbinder JL, Stephenson RC, Dresser MJ, Pitera JW, Scanlan TS, Fletterick RJ (1998) *Biochemistry* 37:5096
- Chae MY, Omburo GA, Lindahl PA, Raushel FM (1993) *J Am Chem Soc* 115:12173
- Omburo GA, Mullins LS, Raushel FM (1993) *Biochemistry* 32:9148
- Omburo GA, Kuo JM, Mullins LS, Raushel FM (1992) *J Biol Chem* 267:13278
- Benning MM, Shim H, Raushel FM, Holden HM (2001) *Biochemistry* 40:2712
- Chen S-L, Fang W-H, Himo F (2007) *J Phys Chem B* 111:1253
- Aubert SD, Li YC, Raushel FM (2004) *Biochemistry* 43:5707
- Ortiz-Hernández ML, Quintero-Ramírez R, Nava-Ocampo AA, Bello-Ramírez AM (2003) *Fun Clin Pharma* 17:717
- Becke AD (1993) *J Chem Phys* 98:1372
- Becke AD (1993) *J Chem Phys* 98:5648
- Lee C, Yang W, Parr RG (1988) *Phys Rev B* 37:785
- Frisch MJ et al (2004) *Gaussian 03, Gaussian, Wallingford*
- Klamt A, Schüürmann G (1993) *J Chem Soc Perkin Trans* 2:799
- Cammi R, Mennucci B, Tomasi J (1999) *J Phys Chem A* 103:9100
- Barone V, Cossi M (1998) *J Phys Chem A* 102:1995
- Tomasi J, Mennucci B, Cammi R (2005) *Chem Rev* 105:2999